Fusion Engineering and Design 9 (1989) 175–180
North-Holland, Amsterdam

THE RFX GRAPHITE TILES: DESIGN AND TESTS

A. DORIA [1], F. ELIO [1], M. FAURI [1], and F. GNESOTTO [2]

[1] *Istituto Gas Ionizzati (Associazione ENEA-CNR-EURATOM), Conso Stati Uniti 4, 35020 Padova, Italy*
[2] *Dipartimento di Ingegneria Elettrica, Università di Padova, Padova, Italy*

The paper, after a brief introduction covering the basic concepts underlying the design of the RFX first wall, describes the main features of the graphite tiles and presents their predicted operating conditions in the presence of applied heat fluxes and electrodynamic forces. On the basis of the results of experimental tests performed to measure the tile-vessel contact conductance, the thermal behaviour is analyzed by means of numerical models which simulate the real operating conditions of the first wall and vacuum vessel, with its forced gas cooling system and its thermal insulation. The safety margin, preventing tile rupture due to electrodynamic extraction forces during fast plasma current terminations, is then investigated by means of mechanical tests closely reproducing the real load distribution. Finally, the stresses due to machining allowances on the tiles and on their grooved seats are analyzed by means of a finite-element model, under the load produced by the bayonet keys which clamp the tiles to the vacuum vessel stiffening rings.

1. Introduction

The RFX [1] first wall (major radius $R = 2000$ mm, inner minor radius $a = 457$ mm) is composed of 2016 trapezoidal graphite tiles (72 in the toroidal direction, 28 in the poloidal direction), covering the whole vacuum vessel surface except for pumping and diagnostic ports. The first wall is only 18 mm thick, due to the need to keep the plasma edge as near as possible to the conducting walls (vacuum vessel and shell) for the purpose of plasma stability [2].

A full graphite armor was chosen for the following reasons:

- a metallic wall with metallic limiters would produce high-Z contamination and could be seriously damaged by heat flux;
- a metallic wall with graphite limiters would produce both high-Z and low-Z contamination (although less than in the case above) which could impair pulse repeatability and interpretation of physics data; the limiters would experience very high heat loads and the metallic wall could also be damaged during badly controlled pulses, such as fast terminations;
- a full graphite wall is considered to be compatible with RFX physics requirements in terms of impurity production and hydrogen recycling properties, and graphite offers excellent thermal shock resistance.

The tiles are individually clamped onto the poloidal rings of the vessel (fig 1), in order to minimize eddy currents and to allow remote manipulation of single tiles. A mechanical attachment (fig. 2) was preferred to a brazed joint since a metal plate would be subject to excessive electrodynamic forces during fast plasma current terminations.

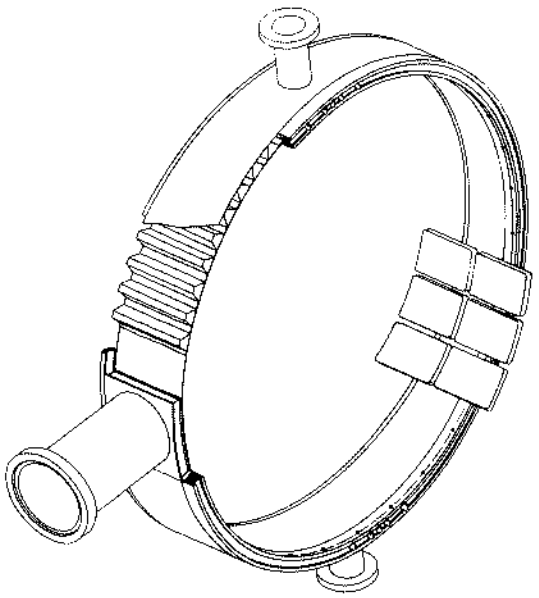

Fig. 1. One of the 72 vessel elements, showing some graphite tiles.

The paper describes the methods and results of numerical and experimental analyses carried out under thermal, electrodynamic, and static loads.

2. Tile design

The tiles are made from Le Carbone-Lorraine 5890 PT graphite. This is a micrograined, high purity, high density, quasi-isotropic graphite, widely used in tokamak experiments [3]. Due to the device's toroidal shape, the tiles are trapezoidal and a number of special tiles are required for the 78 access ports to the torus inside. The vessel rings which support the tiles (fig. 1) are cooled on two sides by a forced flow of nitrogen or carbon dioxide [4], so that the thermal power from the plasma is extracted as closely as possible to the deposition area. This minimizes thermally induced stresses on the vacuum vessel structure.

The clamp is composed (fig. 2) of an Inconel 625 bush, TIG welded to the vessel ring, and of a molybdenum key [5]. A graphite cap is brazed onto the key in order to prevent melting of the exposed surfaces and high-Z plasma contamination.

3. Operating conditions

The cooling and heating systems [4] will keep the vessel wall at an almost constant temperature during the experiments, ranging from approximately 50 to 350 °C. During a full-power pulse (plasma current $I_p = 2$MA, duration $t_p = 0.31$ s) 20 MJ will be deposited on the first wall. Table 1 gives the wall load for the three pulse phases. The assumed poloidal peaking factor of 5 takes account of a 3 cm misalignment between the graphite wall and the plasma outer flux surface, and of an energy scrape-off layer characteristic length of 0.5 cm.

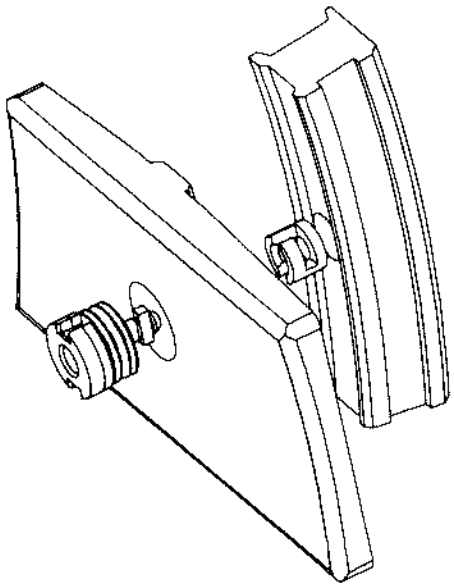

Fig. 2. Exploded view of the tile and its clamp.

Table 1
Thermal load on the first wall

	Duration (ms)	Average power (MW)	Average power density (MW/m^2)	Maximum power density (MW/m^2)
Current rise	30	200	5.5	27
Current flat-top	250	36	1.0	5
Current decay	30	167	4.6	22

As far as mechanical conditions are concerned, sudden plasma current terminations may produce significant eddy currents on first wall components. In RFX, due to the absence of metal backing plates and the fairly low toroidal field, the resultant forces are reasonably low: in the case of an exponential plasma current decay with a time constant as low as 0.1 ms, the peak extraction force for a single tile is less than 75 N, while the torques along the three tile axes are always less than 1.5 N m.

4. Heat conduction to the vessel

The conductive heat exchange from the back of the tile to the vacuum vessel occurs through the curved surface of the tile-supporting rib, which matches the poloidal groove machined in the solid ring of the vacuum vessel (fig. 2). The surface finish and dimensional precision of the mating surfaces strongly affect the value of the contact conductance [6]. For the components tested, the roughness of the tile contact surface is measured as 2 μm, while the roughness of the Inconel surface is less than 0.5 μm.

Measurements of the thermal contact conductance are taken using the stationary temperature gradient method. The front face of the tile is heated by an electrical heater, while the Inconel 625 block is cooled by water (fig. 3). Two thermocouples are inserted into the Inconel block and into the graphite tile as closely to the contact surface as possible.

When the system reaches steady state, and assuming the contact surface is isothermal, the following equation

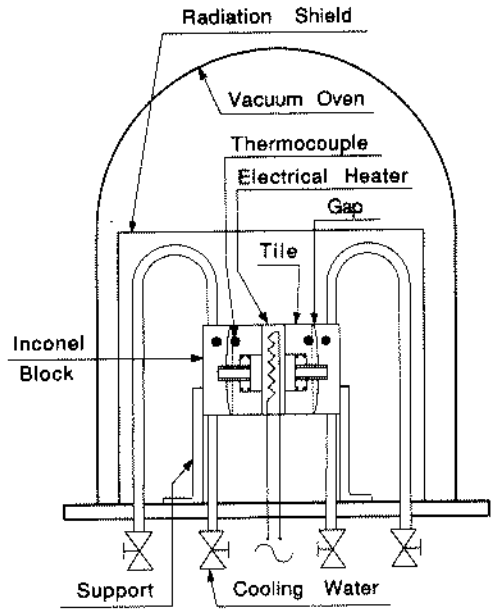

Fig. 3. Experimental apparatus for thermal conductance measurements.

can be written:

$$Q = \frac{A}{\frac{S_g}{\lambda_g} + \frac{1}{h} + \frac{S_i}{\lambda_i}} (T_g - T_i) \qquad (1)$$

where Q is the conductive thermal power which flows from the section of the graphite tile, in which we measure the temperature T_g, to the section of the Inconel 625 block, in which we measure the temperature T_i; A is the contact area; S_g and S_i are the distances from the two measurement sections to the contact surface; λ_g and λ_i are the thermal conductances of graphite and Inconel 625. H is the unknown thermal contact conductance which can be calculated from eq. (1) if T_g and T_i are measured and if Q is known.

Table 2

Thermal contact conductance

W (W)	15.4	20	25
Q_{rad} (W)	2.6	3.7	5
Q (W)	12.8	16.3	20
ΔT (K)	116	155	185
$Q/\Delta T$ (W/K)	0.110	0.105	0.108
h (W/m^{2}K)	74	71	73

Q is smaller than the input power on the tile surface, W, because the tiles exchange heat with the surrounding objects. The vacuum eliminates conductive and convective heat loss to the air; conductive heat flux through solid objects is eliminated, the apparatus being supported outside the measurement section (fig. 3). To reduce radiative heat loss, a symmetrical system has been designed: the electrical heater is placed between the front faces of two tiles, so that all the input power is transferred to the tiles. Finally, the radiation from the back faces of the tiles to the surface of the oven is reduced by using a radiation shield; nevertheless, the power Q_{rad} is estimated by using heat radiation equations [6] and is used to calculate $Q = W - Q_{rad}$.

The test was carried out with a contact pressure of 0.03 MPa (clamping force of 50 N $\pm$ 10 %) and varying the heat flux on the tile surface. The results are summarized in table 2; the margin of error in the measurements of h is about 20%. The linear correlation between Q and ΔT shows that the thermal radiation has been eliminated. The measured value of h agrees well with the results of similar measurements [7,8] and was used for the following thermal analysis.

5. Thermal analysis

The transient thermal load acting on the graphite tiles is shown in table 1. A peak surface temperature of approximately 900 °C is reached during the pulse [10] but, due to the good thermal capacity of graphite, only a small fraction of the tile thickness is subject to significant temperature fluctuations. Consequently, thermal exchange between graphite tile and vacuum vessel can be considerd to be practically stationary. Furthermore, the high surface temperature under the transient load produces an efficient radiative exchange from tile to tile, reducing the temperature differences along the poloidal circumference. Therefore, there is no need to take a peaking factor into account for the first wall cooling and, for a plasma current of 2 MA and a duty cycle of 10 min, an average heat flux of 920 W/m^2 was considered.

Two different operating conditions were examined. In the first, the vessel is cooled by the maximum gas flow permissible to keep the temperature as low as possible (50 °C); due to forced convection, the temperature is uniform within a few degrees [4]. The resultant graphite tile temperature is approximately 150 °C, 55% of the total thermal flux is conducted across the thermal contact, 45% is radiated.

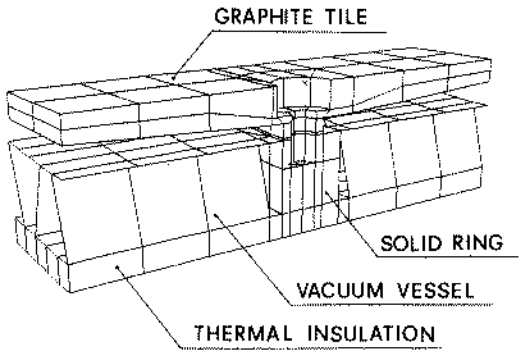

Fig. 4. F.E. mesh for thermal analysis.

On the other hand, to operate at a high wall temperature, the forced cooling is off. In this case, all the thermal power is radially transferred to the thermal insulation of the vessel, which may cause significant thermal gradients across the Inconel sheets. A finite element analysis [9] of the tile and vessel temperature distribution has been performed. The model (fig 4) represents the graphite tile, the vacuum vessel, and the thermal insulation.

The following boundary conditions were considered: heat flux on the front tile surface, radiation between the back of the tile and the vacuum vessel, convection to the ambient air, and radiation to the enclosure at 40 °C from the bottom surface of the thermal insulation. The model takes into account mutual radiation between neighbouring tiles by means of special boundary elements.

The graphite tile shows a fairly uniform temperature of 415 °C, while the vacuum vessel temperature is in the range 390 to 365 °C (fig. 5). Due to the efficiency of radiation, the thermal gradient in the vessel is mainly radial and the conductive flux across the contact between tile and vacuum vessel is only 10%. The temperature difference between inner and outer vessel sheets is acceptable [11].

6. Stress and strength

Stresses on the tiles are induced by electromagnetic loads, clamping forces, and temperature gradients. For those produced by thermal gradients, the operating conditions of the RFX tiles can be compared with those of various high heat flux experiments carried out on free blocks of similar graphites suited to fusion applications [12–15]. It turns out that thicker blocks overcome more severe thermal conditions than in RFX; nevertheless, thermocycling tests are now planned on real components.

6.1. Magnetic load

The ability of the tile to withstand detachment from the wall was experimentally investigated with a rupture test. An apparatus was used to simulate the magnetic pressure on the tile and the retention force of the key. The test was designed to check the tile central zone, in particular, where a large hole is drilled to make room for the head of the key. The apparatus is composed of two hinged rubber beds and a central shaft with a sphere (fig. 6). All the tests performed terminated with the punching of the annular zone under the head of the

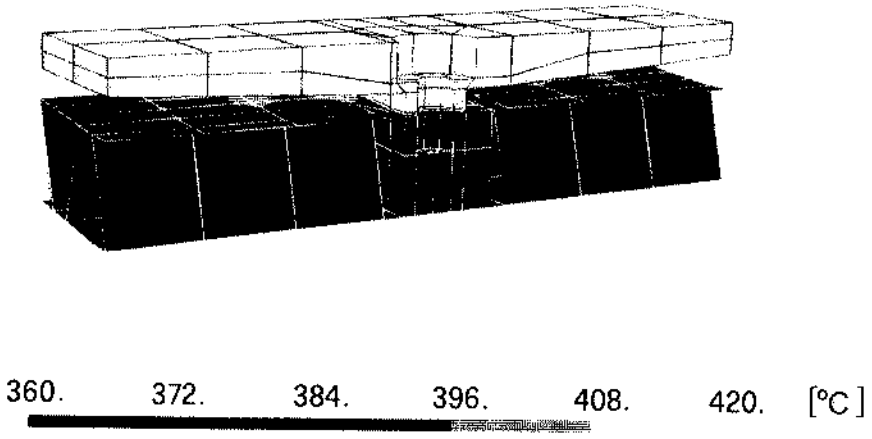

Fig. 5. Temperature distribution without vessel cooling.

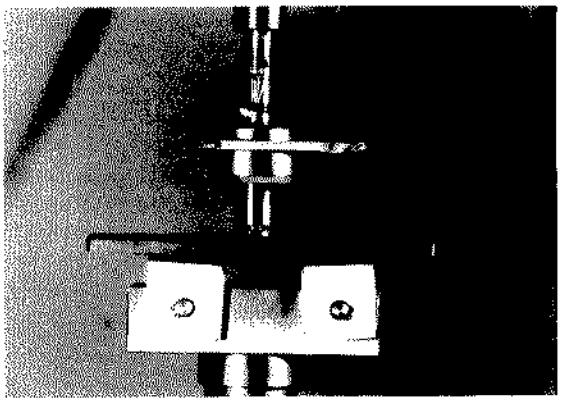

Fig. 6. Experimental apparatus for tile rupture tests.

key (fig. 7); the breaking force was 2.5 kN, which is considered a safe margin for operation.

6.2. Clamping load

The clamping force should in principle not be dangerous for the tile since it induces compressive stress above all. However, geometric imperfections in the contact with the vessel rings cannot be excluded, which may cause tensile stresses. In fact, in order to avoid uncertainties in tile positioning, machining allowances have been set to ensure that the outer regions of the tile rib always match the ring. Due to the difference in radius of curvature, a gap of 0.05 mm may occur between the tile centre and the seat. In this case, the tile will bend when subject to the clamping force or when accidentally pressed against the ring by the manipulator. A finite element analysis [16] of the tile has been carried out to evaluate the maximum tensile stress arising in the tile up to the full contact with the seat.

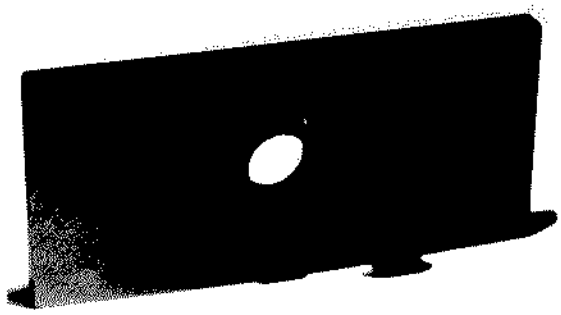

Fig. 7. One tile after rupture test.

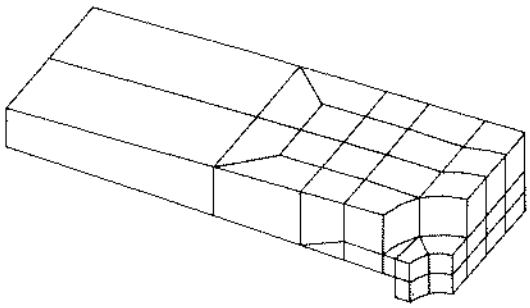

Fig. 8. F.E. mesh for mechanical analysis.

Fig. 8 shows the mesh of the tile, reduced to a quarter due to the symmetries: the mesh is finer in the central zone, where stress distribution is complicated by the presence of the hole.

The stress distribution in the central region is illustrated in fig. 9 (arrows = tensile stress). The tensile stress is relatively high around the hole; nevertheless, the maximum value reached for a deflection of 0.05 mm, corresponding to a force of 700 N, is about 11 MPa; the flexural strength of the material is higher than 40 MPa. Moreover, neither the clamping key, nor the manipulator, are able to apply such a large force on the centre of the tile.

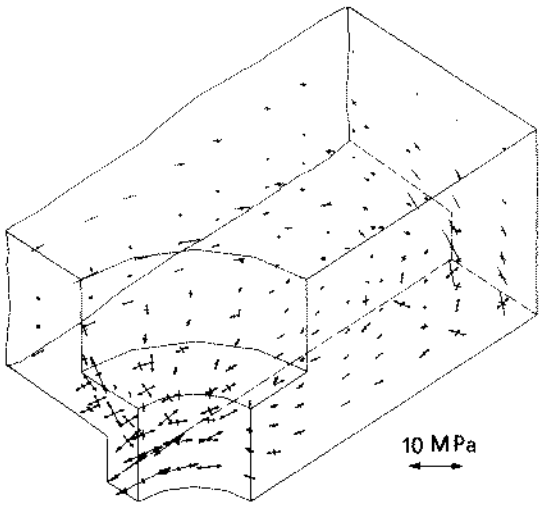

Fig. 9. Stress distribution around the central hole.

7. Conclusions

The results of finite-element analyses and experimental tests reported in this paper show that the RFX graphite tile design is very reliable mechanically, and operates within reasonable safety margins under all the predicted load conditions. The cooling system allows operation of the machine at different wall temperatures without producing dangerous secondary stresses on the structure of the vacuum vessel. It will therefore be possible to change the graphite properties with regard to particle recycling and impurity production, as required by the experimental physics.

Acknowledgement

The authors wish to acknowledge the assistance of G. Mella, C. Sardo, and F. Vicari in performing the experimental tests.

References

[1] G. Malesani and G. Rostagni, The RFX Experiment, Proc. 14th Symp. on Fusion Technology, Avignon, 1986, pp. 173–184.
[2] H.A.B. Bodin and A.A. Newton, Reversed field pinch research, Nucl. Fusion 20, no. 10 (1980) 1255–1324.
[3] P. Deschamps, J. Dietz and M. Yvars, Fabrication and characterization of graphite 5890 PT limiters used in TFR and JET tokamaks, Proc. 13th Symp. on Fusion Technology, Varese, 1984, pp. 1243–1246.
[4] F. Elio and M. Fauri, The heating and cooling systems of the RFX vessel, Proc. 12th Symp. on Fusion Engineering, Monterey, 1987, to appear.
[5] A. Doria and F. Elio, Development of a first wall clamp for remote handling, Fusion Engrg. Des. 8–10 (1989), in there Proceedings.
[6] W.M. Rohsenow, J.P. Hartnett and E.M. Ganic', Handbook of Heat Transfer Fundamentals, second edition, (McGraw Hill, New York, 1985).
[7] K. Ioki et al., Thermomechanical behaviour of graphite and coating materials subjected to a high heat flux, Fusion Eng. Des. 5 (1987) 181–186.
[8] D.W. Doll and E. Reis, Thermal contact conductance measurements on Doublet III armor tile graphite, Proc. 10th Symp. on Fusion Engineering, Philadelphia, 1983, pp. 1099–1102.
[9] MacNeal Schwendler Corp., MSC NASTRAN, Version 64A, (Los Angeles).
[10] F. Elio, F. Gnesotto, R.M. Pauletti and P. Sonato, Performance analysis of a full graphite armor for RFX, Proc. 14th Symp. on Fusion Technology, Avignon, 1986, pp. 513–519.
[11] F. Elio, C. Majorana, P. Zaccaria and F. Zaupa, Structural and thermal analysis of the RFX vacuum vessel, Proc. 11th Symp. on Fusion Engineering, Austin, 1985, pp. 825–829.
[12] J.B. Whitley, Material considerations for high heat flux components, J. Nucl. Mater. 133&134 (1985) 39–45.
[13] M. Shibui et al., Thermal shock behavior of first wall material candidates, Proc. 11th Symp. on Fusion Engineering, Austin, 1985, pp. 877–880.
[14] J. Bohdansky, C.D. Croessmann and J. Linke, Behaviour of graphites under intense heat loads, Proc. 14th Symp. on Fusion Technology, Avignon, 1986, pp. 1063–1068.
[15] H. Brinkschulte, E. Deksnis and A.S. Bransden, Heat shock resistance of graphite determined with a CO_2 laser, JET report, JET-P (87) 43 (1987).
[16] ADINA Engineering AB, ADINA-A finite element program for Automatic Dynamic Incremental Nonlinear Analysis, (Sweden).